Naphtho[2,1-b:6,5-b′]difuran: A Versatile Motif Available for Solution-Processed Single-Crystal Organic Field-Effect Transistors with High Hole Mobility

Chikahiko Mitsui,[†,‡] Junshi Soeda,[‡] Kazumoto Miwa,[‡] Hayato Tsuji,*[,†] Jun Takeya,*[,‡] and Eiichi Nakamura*[,†]

[†]Department of Chemistry, School of Science, The University of Tokyo, Hongo, Bunkyo-ku, Tokyo 113-0033, Japan
[‡]ISIR, Osaka University, 8-1 Mihogaoka, Ibaraki, Osaka 567-0047, Japan

Ⓢ *Supporting Information*

ABSTRACT: We here report naphtho[2,1-b:6,5-b′]-difuran derivatives as new p-type semiconductors that achieve hole mobilities of up to 3.6 cm^2 V^{-1} s^{-1} along with high I_{on}/I_{off} ratios in solution-processed single-crystal organic field-effect transistors. These features originate from the dense crystal packing and the resulting large intermolecular π-orbital overlap as well as from the small reorganization energy, all of which originate from the small radius of an oxygen atom.

Furan[1,2] is a ubiquitous organic frame found in nature and synthetically readily accessible, yet it has received far less attention than thiophenes in organic electronics research,[3−5] particularly in device applications, which include one example of an organic light-emitting diode (OLED)[6] and some examples of organic field-effect transistors (OFETs)[7,8] and organic photovoltaic (OPV) devices.[9] This lack of interest could have arisen because of some earlier examples that showed instability under oxidative conditions.[10] We conjectured that the use of a fused furan skeleton, such as in **DPBDF** (Scheme 1), would exhibit not only stability but also p-type semi-conducting properties. Indeed, amorphous films of some benzodifuran (**BDF**) derivatives showed carrier mobilities of >10^{-3} cm^2 V^{-1} s^{-1}, which is high for amorphous materials, using the time-of-flight technique.[11] We also demonstrated that a new ambipolar **BDF** led us to develop a unique homojunction
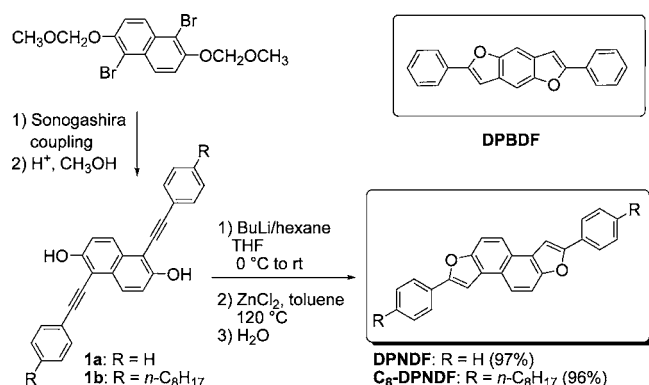
OLED device.[12] To our disappointment, however, **BDF**s performed rather poorly in single-crystal OFET devices, probably because of poor charge injection due to the low HOMO level and poor intermolecular interactions. We report here that naphtho[2,1-b:6,5-b′]difuran (**NDF**) serves as a novel and effective motif for single-crystal OFETs made by a solution- and vapor-growth method, which show carrier mobilities of up to 3.6 cm^2 V^{-1} s^{-1} as well as high I_{on}/I_{off} ratios—values among the highest for solution-processed OFETs.[13] Such high performance of the **NDF**-based OFETs illustrates the potential of furans in organic electronics applications, which needs to be explored further in the future.[14]

Among the **NDF** derivatives we examined, two were found to have the optimum structure for control of the solubility and device processability. We synthesized **DPNDF** and its octyl-substituted derivative **C$_8$-DPNDF** in excellent yields by a zinc-mediated double-cyclization reaction of dialkynes **1a** and **1b**, respectively (Scheme 1).[11,12,15]

We first fabricated bottom-gate−top-contact OFETs by the oriented-crystal-growth method[13] using **C$_8$-DPNDF** and found that the devices showed excellent performance. We employed the octyl group to achieve high solubility of the compound while maintaining the crystallinity. Thus, a droplet of a 0.2 wt% solution of **C$_8$-DPNDF** in chlorobenzene was placed at an edge of a liquid-sustaining piece on a substrate, so that the crystalline domain would grow in the direction of evaporation of the solvent.[13] As examined for four devices, this single-crystalline film exhibited FET mobilities of 1.5−3.6 cm^2 V^{-1} s^{-1} in the saturation regime with a high I_{on}/I_{off} ratio of 10^4−10^5 and a threshold voltage of −100 V (Figure 1 for device **A**, which showed the highest mobility).

The molecular orientation and homogeneity of the solution-grown **C$_8$-DPNDF** film (Figure 2a) were determined by X-ray diffraction (XRD) measurements (Figure 2b) and atomic force microscopy (AFM) (Figure 2c,d). The XRD data revealed that the c axis is oriented perpendicular to the substrate and the *ab* plane (the carrier conduction path) parallel to the substrate [Figure 2b; also see the Supporting Information (SI)]. The AFM images revealed only a few steps corresponding to a single molecular height, indicating the homogeneity of the film, which bears a molecularly flat area extending to a micrometer area.

Scheme 1

1) Sonogashira coupling
2) H$^+$, CH$_3$OH

1) BuLi/hexane
   THF
   0 °C to rt
2) ZnCl$_2$, toluene
   120 °C
3) H$_2$O

DPBDF

1a: R = H
1b: R = n-C$_8$H$_{17}$

DPNDF: R = H (97%)
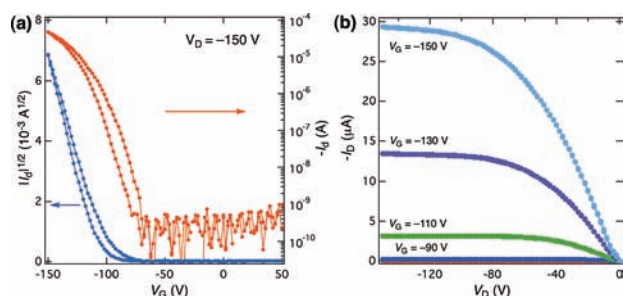**C$_8$-DPNDF**: R = n-C$_8$H$_{17}$ (96%)

Figure 1. OFET characteristics of **C₈-DPNDF**: (a) transfer and (b) output characteristics of device **A**.
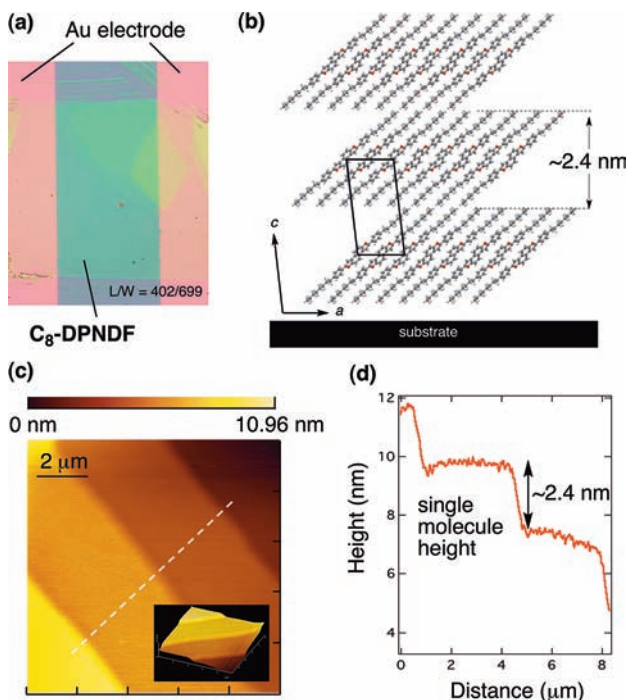

Figure 2. Molecular orientation and homogeneity of the solution-grown single crystal of **C₈-DPNDF**. (a) Photograph of a representative OFET device. (b) Schematic illustration of the packing diagram of **C₈-DPNDF** along the *b* axis as revealed by XRD. The parallelogram stands for a unit cell. (c) Top view of the AFM image (inset: bird's-eye view). (d) Cross-sectional AFM profile along the white dotted line in (c). The observed 2.4 nm height of a step agrees very well with the step size shown in (b).

Interestingly, the parent compound **DPNDF** showed an OFET behavior similar to that of **C₈-DPNDF** regardless of the fabrication process. We first examined physical vapor transport (PVT) to prepare single crystals of **DPNDF**. The platelet single crystals thus obtained were manually laminated on surface-treated [using a fluorinated self-assembled monolayer (F-SAM)][16] Si/SiO₂ substrates with patterned Au electrodes to construct a bottom-gate−bottom-contact architecture. The transfer and output characteristics of the **DPNDF**-laminated device **B** are plotted in Figure 3. This device showed a hole mobility of 1.3 cm² V⁻¹ s⁻¹ in the saturation regime with a high I_{on}/I_{off} ratio of 10⁵. The hole mobility of **DPNDF** is 1.6 times higher than that of a thiophene analogue having exactly the same carbon framework.[17] It is noteworthy that the threshold voltage of the laminated device was −10 V. This significantly large shift of the threshold voltage to the positive side can be ascribed to the use of F-SAM.[16] The solution-processed OFET
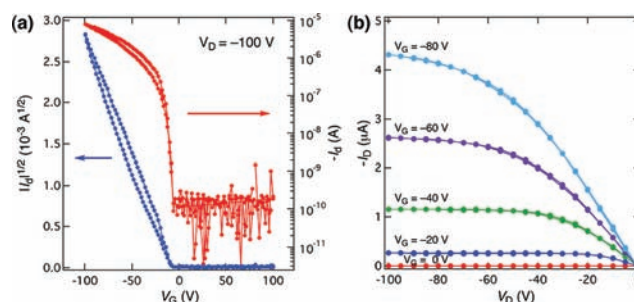

Figure 3. Representative characteristics of a PVT-grown single-crystal OFET using **DPNDF** (device **B**): (a) transfer and (b) output characteristics.

(device **C**) was also fabricated by vaporizing solvent on an inclined substrate (as for device **A**) using a 0.2 wt % solution of **DPNDF** in *o*-dichlorobenzene at 150 °C to form a single crystal on the surface-treated Si/SiO₂ substrate. This solution-crystallized OFET device **C** showed similar characteristics as device **B** and a mobility of 1.0 cm² V⁻¹ s⁻¹ (for details, see the SI).

It is intriguing that the **DPNDF** derivatives showed high hole mobility, and we examined its origin in some detail. Calculated transfer integrals (t) among HOMOs in a crystal of the **NDF** molecules provided support for these characteristics (Figure 4).
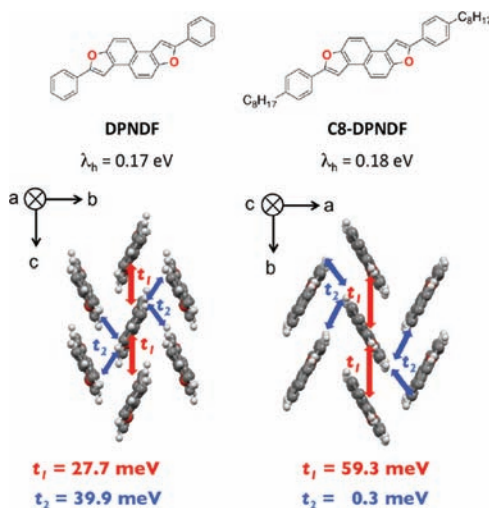

Figure 4. Crystallographic axes in the **NDFs** and the transfer integrals calculated using the ADF program. For **C₈-DPNDF**, the alkyl groups have been omitted for clarity.

The transfer integrals for **C₈-DPNDF** are highly anisotropic, with very high values for one direction (t_1 = 59.3 meV and t_2 = 0.3 meV along the stacking and transverse directions, respectively).[18] We consider that the perpendicular positional relationship between the molecules along the transverse direction is responsible for this t_2 value. The t_1 value for the stacking direction is slightly larger than that for 2,7-dioctyl[1]-benzothieno[3,2-*b*][1]benzothiophene (**C₈-BTBT**) (57 meV for the stacking direction and 41 meV for the transverse direction),[17] which shows a very high carrier mobility.[19] On the basis of these data, we could expect that there should be room to achieve a hole mobility higher than those observed herein for the **C₈-DPNDF**-based OFETs. We consider the mobility in the present case to be limited by a nonideal crystal orientation in the solution-crystallized device, as the crystal structure of the

solution-crystallized C_8-**DPNDF** film indicated that the crystal growth direction (along which the source–drain channel was constructed) was not completely parallel to the stacking direction (i.e., the *b* axis) but ca. 20–30° from the *b* axis. Hence, we expect that once the channel direction is optimized for C_8-**DPNDF**, the mobility will be further improved.

The transfer integrals for **DPNDF** along the stacking and transverse directions are t_1 = 27.7 meV and t_2 = 39.9 meV, respectively, as calculated on the basis of the experimental packing parameters in a single crystal.[18] Notably, these values are much higher than those for the thiophene counterpart[17] (11 and 9 meV, respectively). XRD analysis of the PVT-grown single-crystal OFET of **DPNDF** (device **C**) revealed that the channel direction of our device was almost parallel to the transverse direction, which has a large transfer integral (see the SI), and hence, the experimental mobility data obtained for device **C** should reflect the best carrier mobility of a **DPNDF** single crystal.

It should be noted that the **DPNDF** and C_8-**DPNDF** molecules in single crystals stack in a herringbone manner (Figure 4) with a shortest intermolecular distance of 2.80 Å. The thiophene counterpart also packs in a herringbone manner, and the shortest intermolecular distance is longer (3.31 Å) because of the larger atomic radius of a sulfur atom (1.80 Å) than of an oxygen atom (1.52 Å). The **NDF** molecules are more densely packed in a single crystal, which could be partially responsible for the large transfer integrals of **NDF**s.

The reorganization energy serves as a measure to estimate the charge carrying ability in the solid.[20] The reorganization energies for hole formation (λ_h) in **DPNDF** and C_8-**DPNDF** are 0.17 and 0.18 eV, respectively, as calculated for a single molecule at the B3LYP/6-31G* level.[21] These values are smaller than those for the sulfur analogue **DPNDT**[17] (0.19 eV) and α-oligofurans (0.23–0.37 eV),[22] which supports the high ability for carrier transportation by **DPNDF** and C_8-**DPNDF**. The expanded π-electron conjugation of the naphthalene motif contributes to the small reorganization energy.

The **NDF**s are both thermally stable (TGA traces are shown in Figure S1 in the SI) and electrochemically stable. Cyclic voltammograms for the **NDF**s showed reversible oxidation waves (Figure S2). Notably, α-unsubstituted furans generally exhibit irreversible oxidation waves and may lead to electrochemical polymerization.[23] The half-oxidation potential of **DPNDF** is 0.68 V vs Fc/Fc$^+$, from which we estimate the HOMO energy level to be −5.48 eV.[24] C_8-**DPNDF** showed a slightly lower oxidation potential of 0.62 V vs Fc/Fc$^+$ because of the electron-donating alkyl chains, and the HOMO energy level was estimated to be −5.42 eV. These HOMO energy levels would allow smooth hole injection into the **NDF**, which would then serve as a viable p-type organic semiconductor.

In conclusion, we have found that two furan units fused by a naphthalene serve as stable p-type organic semiconductors for OFET devices with high mobility. The **NDF**s rival the hitherto known high-performance materials for hole-transporting ability in the crystalline state. The solution-grown single-crystal devices using C_8-**DPNDF** showed hole carrier mobilities of up to 3.6 cm^2 V^{-1} s^{-1}, which could be improved by careful control of the processing direction.

ASSOCIATED CONTENT

Ⓢ Supporting Information
Experimental details, thermal data, electrochemical measurements, FET fabrication and evaluation, complete ref 21, and

crystallographic data (CIF). This material is available free of charge via the Internet at http://pubs.acs.org.

■ AUTHOR INFORMATION

Corresponding Author
tsuji@chem.s.u-tokyo.ac.jp;　takeya@sanken.osaka-u.ac.jp; nakamura@chem.s.u-tokyo.ac.jp

Notes
The authors declare no competing financial interest.

■ ACKNOWLEDGMENTS

■ REFERENCES

(1) For recent reviews, see: (a) Boto, A.; Alvarez, A. Furan and Its Derivatives. In *Heterocycles in Natural Product Synthesis*; Majumdar, K. C., Chattopadhyay, S. K., Eds.; Wiley-VCH: Weinheim, Germany, 2011; pp 99−152. (b) Bunz, U. H. F. *Angew. Chem., Int. Ed.* **2010**, *49*, 5037. (c) Brown, R. C. D. *Angew. Chem., Int. Ed.* **2005**, *44*, 850.

(2) For the chemical synthesis of α-oligofurans, see: Gidron, O.; Diskin-Posner, Y.; Bendikov, M. *J. Am. Chem. Soc.* **2010**, *132*, 2148.

(3) (a) Müllen, K.; Scherf, U. *Organic Light-Emitting Devices: Synthesis, Properties and Applications*; Wiley-VCH: Weinheim, Germany, 2006. (b) Shinar, J. *Organic Light-Emitting Devices: A Survey*; Springer: New York, 2004. (c) Li, Z.; Meng, H. *Organic Light-Emitting Materials and Devices*; CRC Press: Boca Raton, FL, 2007.

(4) Sun, S.-S.; Sariciftci, N. S. *Organic Photovoltaics: Mechanism, Materials, and Devices*; CRC Press: Boca Raton, FL, 2005.

(5) *Handbook of Thiophene-Based Materials: Applications in Organic Electronics and Photonics*; Perepichka, I. F., Perepichka, D. F., Eds.; Wiley: Chichester, U.K., 2009.

(6) For OLEDs using furan-containing materials, see: Wu, C.-C.; Hung, W.-Y.; Liu, T.-L.; Zhang, L.-Z.; Luh, T.-Y. *J. Appl. Phys.* **2003**, *93*, 5465.

(7) For OFETs using furan-containing materials, see: (a) Miyata, Y.; Nishinaga, T.; Komatsu, K. *J. Org. Chem.* **2005**, *70*, 1147. (b) Miyata, Y.; Terayama, M.; Minari, T.; Nishinaga, T.; Nemoto, T.; Isoda, S.; Komatsu, K. *Chem.—Asian J.* **2007**, *2*, 1492.

(8) For OFETs using oligofurans, see: Gidron, O.; Dadvand, A.; Sheynin, Y.; Bendikov, M.; Perepichka, D. F. *Chem. Commun.* **2011**, *47*, 1976.

(9) For OPVs using furan-containing materials, see: (a) Woo, C. H.; Beaujuge, P. M.; Holcombe, T. W.; Lee, O. P.; Fréchet, J. M. J. *J. Am. Chem. Soc.* **2010**, *132*, 15547. (b) Beaujuge, P. M.; Fréchet, J. M. J. *J. Am. Chem. Soc.* **2011**, *133*, 20009. (c) Yiu, A. T.; Beaujuge, P. M.; Lee, O. P.; Woo, C. H.; Toney, M. F.; Fréchet, J. M. J. *J. Am. Chem. Soc.* **2012**, *134*, 2180.

(10) Distefano, G.; Jones, D.; Guerra, M.; Favaretto, L.; Modelli, A.; Mengoli, G. *J. Phys. Chem.* **1991**, *95*, 9746 and references cited therein.

(11) Tsuji, H.; Mitsui, C.; Ilies, L.; Sato, Y.; Nakamura, E. *J. Am. Chem. Soc.* **2007**, *129*, 11902.

(12) Tsuji, H.; Mitsui, C.; Sato, Y.; Nakamura, E. *Adv. Mater.* **2009**, *21*, 3776.

(13) (a) Uemura, T.; Hirose, Y.; Uno, M.; Takimiya, K.; Takeya, J. *Appl. Phys. Exp.* **2009**, *2*, No. 111501. (b) Soeda, J.; Hirose, Y.; Yamagishi, M.; Nakao, A.; Uemura, T.; Nakayama, K.; Uno, M.; Nakazawa, Y.; Takimiya, K.; Takeya, J. *Adv. Mater.* **2011**, *23*, 3309.

(14) While we were preparing this manuscript, a linear NDF isomer (2,7-diphenylnaphtho[2,3-*b*:6,7-*b'*]difuran) and its thiophene and selenophene counterparts were reported. See: Nakano, M.; Mori, H.; Shinamura, S.; Takimiya, K. *Chem. Mater.* **2012**, *24*, 190.

(15) (a) Tsuji, H.; Yokoi, Y.; Mitsui, C.; Ilies, L.; Sato, Y.; Nakamura, E. *Chem.—Asian J.* **2009**, *4*, 655. (b) Tsuji, H.; Mitsui, C.; Sato, Y.; Nakamura, E. *Heteroat. Chem.* **2011**, *22*, 316. (c) Tsuji, H.; Favier, G. M. O.; Mitsui, C.; Lee, S.; Hashizume, D.; Nakamura, E. *Chem. Lett.* **2011**, *40*, 576.

(16) Kobayashi, S.; Nishikawa, T.; Takenobu, T.; Mori, S.; Shimoda, T.; Mitani, T.; Shimotani, H.; Yoshimoto, N.; Ogawa, S.; Iwasa, Y. *Nat. Mater.* **2004**, *3*, 317.

(17) Shinamura, S.; Osaka, I.; Miyazaki, E.; Nakao, A.; Yamagishi, M.; Takeya, J.; Takimiya, K. *J. Am. Chem. Soc.* **2011**, *135*, 5024.   In this paper, a thin-film OFET using 2,7-diphenylnaphtho[2,1-*b*:6,5-*b*′] dithiophene was reported to show a mobility of 0.8 cm^2 V^{-1} s^{-1}.

(18) The transfer integrals were calculated using the PW-91 TZP package in the Amsterdam Density Functional (ADF) program. See: *Amsterdam Density Functional (ADF) Users Guide*, release 1.1; Department of Theoretical Chemistry, Free University Amsterdam: Amsterdam, The Netherlands, 1994.

(19) Minemawari, H.; Yamada, T.; Matsui, H.; Tsutsumi, J.; Haas, S.; Chiba, R.; Kumai, R.; Hasegawa, T. *Nature* **2011**, *475*, 364.

(20) (a) Marcus, R. A. *Rev. Mod. Phys.* **1993**, *65*, 599. (b) Brédas, J. L.; Calbert, J. P.; da Silva Filho, D. A.; Cornil, J. *Proc. Natl. Acad. Sci. U.S.A.* **2002**, *99*, 5804.

(21) MO calculations were performed with the DFT method at the B3LYP/6-31G* level using the Gaussian 03 program package. See: Frisch, M. J.; et al. *Gaussian 03*, revision B.05; Gaussian, Inc.: Wallingford, CT, 2004.

(22) Mohakud, S.; Andrews, A. P.; Pati, S. K. *J. Phys. Chem. C* **2010**, *114*, 20436.

(23) Politis, J. K.; Nemes, J. C.; Curtis, M. D. *J. Am. Chem. Soc.* **2001**, *123*, 2537.

(24) We estimated the HOMO energy level (E_{HOMO}) according to the following equation: E_{HOMO} [eV] = − (4.8 + E_{ox} [V]), where E_{ox} is the oxidation potential vs Fc/Fc$^+$ obtained from CV measurements. See: Cardona, C. M.; Li, W.; Kaifer, A. E.; Stockdale, D.; Bazan, G. C. *Adv. Mater.* **2011**, *23*, 2367.